12WCEE 2000

EFFECTS OF VALLEY SHAPE ON SEISMIC RESPONSES OF FILL DAMS

Masukawa SUSUMU[1], Yasunaka MASAMI[2], Asano ISAMU[3] And Tagashira HIDEKAZU[4]

SUMMARY

The study of the seismic behavior during an earthquake and earthquake resistant designs of fill dams is normally performed by means of two-dimensional analysis on the maximum cross section of the dam bodies. The seismic behavior of a fill dam, however, is substantially affected by the valley shape. This paper discusses the three dimensional vibration mode of a fill dam body obtained from shaking table tests using elastic dam models made of silicone rubber. The shape of the vibration modes in particular is studied with regard to deformation. The ratios (L/H) of the crest length (L) to the dam height (H) of the three elastic dam models were 2, 4, and 6. The dam heights were identical but they featured three differing crest lengths. The deformation of the vibration modes was recorded by a high speed video camera. These shaking table models were simulated by means of a computer code for three-dimensional seismic response analysis based on a mode superposition method developed by the authors. The deformation patterns and frequency properties obtained from the tests and those obtained from numerical analysis were compared. The results obtained from the shaking table tests and the numerical analyses have revealed that the vibration properties in the $L/H = 2$ case differ from those in the cases of models with $L/H = 4$ and 6, and that it is necessary to perform three-dimensional seismic response analysis in order to study the seismic behavior of a dam whose L/H is smaller than $L/H = 2$ to 4.

INTRODUCTION

There are 1,517 large fill dams for irrigation in Japan. Those of $L/H = 4$ are the most and those of $L/H = 3$ are second, as shown in Figure 1. L/H is the ratio that obtained by dividing the crest length (L) by the dam height (H). Fill dams constructed at such a relatively narrow valley account for 37%. The results of seismic observations indicating that the topographical features of complex narrow dam sites do effect the seismic behavior of fill dams have also been obtained [Masukawa et. al., 1996]. Research has also been undertaken using numerical analysis to study the effects of valley shape on the dynamic response of fill dams [Majia and Seed, 1983]. But no research on the shape of vibration modes produced by the effects of valley shape has been undertaken with regard to deformation.

This paper describes a study of the effects of valley shape on the seismic behavior of fill dam based on the deformation patterns of the vibration modes. In particular, the effects of the topographical features of a dam site on the deformation pattern of the vibration mode have been clarified by shaking table tests of three elastic dam models made of silicon rubber. They have the identical dam height, but have three different dam crest length. Based on these shaking table tests, the vibration modes were clarified with regard to deformation in order to investigate the effects of the valley shape. Three-dimensional seismic response analysis based on the mode superposition method was performed to determine if it is possible to simulate the dynamic behavior characteristics of the elastic dam models.

SHAKING TABLE TESTS OF ELASTIC DAM MODELS

For along time, dam models used for shaking table tests had been made of agar-agar or gelatin,

[1] *National Research Institute of Agricultural Engineering, Tsukuba, Japan Email: susumu@nkk.affrc.go.jp*
[2] *National Research Institute of Agricultural Engineering, Tsukuba, Japan*
[3] *National Research Institute of Agricultural Engineering, Tsukuba, Japan*
[4] *National Research Institute of Agricultural Engineering, Tsukuba, Japan*

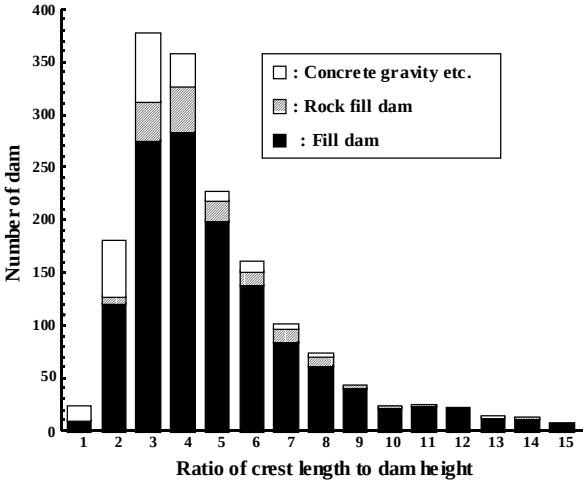

Figure 1: Number of large dam for the ratio of crest length to dam height about dam type

but high polymer silicone rubber has come into use in recent years. The silicon rubber used for these models was extremely stable after hardening. It is necessary to conform to the model rule when performing a model experiment, but it is actually extremely difficult to perform a shaking table test that fully satisfies all conditions necessary for conformity with the model rule. Because the purpose of the elastic dam model testing was to study differences in the vibration mode and deformation pattern caused by the effects of the valley shape, the Young's modulus was set as low value as possible so that these properties could be observed easily. The Young's modulus for the silicon rubber was 39.2 kN/m^2 which is the smallest value possible with this material. The material properties revealed by material testing of the silicon rubber were a unit weight of 9.51 kN/m^3 and a Young's modulus ranging from 36.3 to 65.7 kN/m^2.

As fig. 1 indicates, most large dams for irrigation have L/H of 4. Considering this fact, three models with L/H of 2, 4, and 6 respectively were prepared. Hereafter in this paper the L/H = 2 model, L/H = 4 model, and L/H = 6 model will be abbreviated as L/H = 2, L/H = 4, and L/H = 6 respectively. Because only the effects of the valley shape were to be studied, all three models featured the identical slope gradient and dam height with only the dam crest length different. Consequently, their maximum cross section shapes were also identical. The actual dimensions of the models were: dam height of 30 cm, dam crest lengths of 60 cm (L/H = 2), 120 cm (L/H = 4), and 180 cm (L/H = 6), slope gradient of 1:2.5, and width in the upstream-downstream direction of 155 cm.

Figure 2 presents the maximum cross section that is the same shape of all the three models and Figure 3 presents an outline of the longitudinal section of the models. Figure 4 shows a birds-eye view of L/H = 4. The dots in the figures indicate the locations of accelerometers. These accelerometers were arranged to investigate the amplification of the response acceleration in the dam height direction and the effects of the binding force of the abutment in the longitudinal direction. The locations of the three measurement points on the dam crests of the models where accelerometers were installed are defined as the center (TC), the closer part to the center (TE), and the closer part to the abutment (TB). In the remainder of this paper, these three measurement points are abbreviated as TC, TE, and TB. The accelerometers were strain gauge type uni-directional seismic ones.

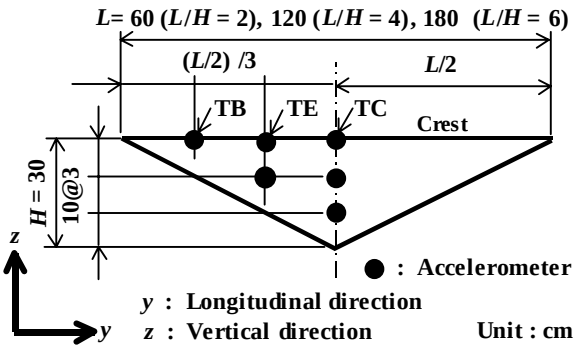

Figure 2: Cross section of elastic dam model

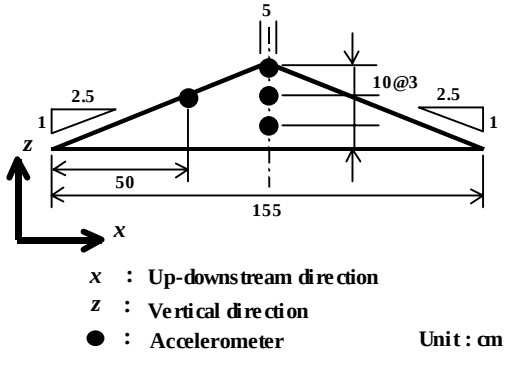

Figure 3: Longitudinal section of elastic dam model

The high speed video camera system measured the vibration modes and deformation patterns. In order to make clear of the deformation of the dam body during the vibration, markers were placed at 10 cm intervals on the dam axis on the crest of each model. Based on the images obtained by the camera, the displacement of the deformation measurement markers referred to above between each frame measured in the vibration mode of the natural frequency. Multi-strobe photography using a 35 mm single lens reflex camera under multi-strobe lighting was performed to confirm the vibration modes.

Figure 4: Bird's-eye view of elastic dam model (L/H = 4)

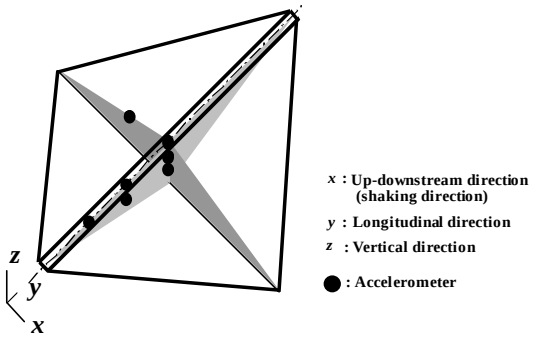

First, vibration with a sweep frequency of a sine wave with constant acceleration amplitude was performed in order to measure the natural frequencies of each model. The acceleration amplitudes were set at 25, 50, 100, and 200 Gal. The sweep frequency ranged from 1 to 30 Hz. Then vibration was performed with the sine wave of the above acceleration amplitudes for the lowest of the natural frequencies obtained from the sweep frequency tests. The only vibration direction was the upstream-downstream direction of the models.

Photograph 1 shows the models installed on the shaking table.

Photograph 1: Appearance of elastic dam models

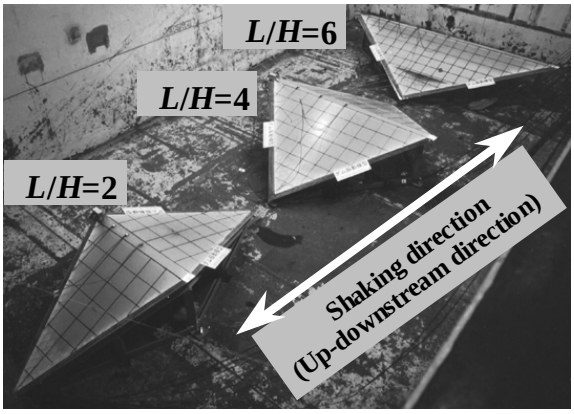

TEST RESULTS

Here, the value obtained by dividing the recorded maximum response acceleration during the sweep frequency tests by the input acceleration was defined as the amplification ratio of acceleration. The resonance curve was obtained from this amplification ratio and the sweep frequency. Figures 5, 6 and 7 show the resonance curves at TC of the each model under the four different input accelerations. Figures 8, 9 and 10 each show the resonance curves at three measurement points (TC, TE, and TB) on the dam crests of each of the models during input of 200 Gal.

Figs 5, 6 and 7 confirm that as the input acceleration rises, the amplification ratio of acceleration also rises. At vibrations of 25 and 50 Gal, because of the lowness of the input acceleration, there are some cases where the precision of the shaking table control is poor and the amplification ratio is not proportional to the size of the input acceleration. At frequencies of 10 Hz or lower, all models display similar frequency properties regardless of the size of the input accelerations. In addition, the most dominant peak occurs at the same frequency regardless of the size of the input accelerations. These results indicate that the silicon rubber used to make the models is an elastic body that is independent of the size of the input acceleration. In the order L/H = 6, 4, and 2, the amplification ratio increases at frequencies other than the natural frequency. It also shows that in L/H = 2 in particular, compared with the other two models, the amplification ratio is large near 10 Hz.

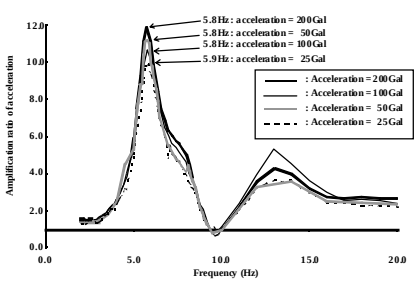

Figure 5: Resonance curves at the center of dam crest (L/H = 6: TC)

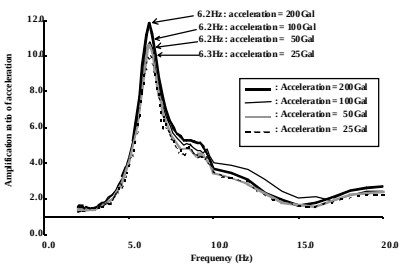

Figure 6: Resonance curves at the center of dam crest (L/H = 4: TC)

Figure 7: Resonance curves at the center of dam crest (*L*/*H* = 2: TC)

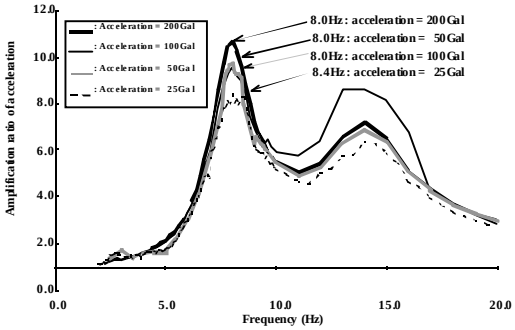

The resonance curves at TC shown in figure 8 confirm that the natural frequency of the 1st mode in *L*/*H* = 2 indicates higher frequency than the almost identical the natural frequency of the 1st mode in both *L*/*H* = 4 and *L*/*H* = 6. The natural frequencies of the 1st mode in each model do not indicate a proportional relationship to each *L*/*H*. From this result, it is assumed that from *L*/*H* = 4 to *L*/*H* = 2, as the dam crest length declines, the effects of the binding force of the abutment appear abruptly. The resonance curves for TE shown in figure 9 indicate that in *L*/*H* = 6 and *L*/*H* = 4, the amplification ratio at the natural frequencies of the 2nd mode of 8.4 Hz in the former case and 10.0 Hz in the latter case are larger than that at those of the 1st mode. In *L*/*H* = 2, a clear dominant peak is not revealed in the frequencies higher than the 1st mode with only a slight peak confirmed at 13.0 Hz. The resonance curves in *L*/*H* = 2 differ from those in *L*/*H* = 6 and *L*/*H* = 4. The natural frequency of the 1st mode at TE in *L*/*H* = 2 indicates a frequency almost identical to the natural frequency of the 1st mode at TC. This reveals that in the case of *L*/*H* = 2, large vibration occurs at TE in the natural frequency of the 1st mode at TC. The resonance curves at TB shown in figure 10 indicate that the resonance curves in *L*/*H* = 2 differ from those in *L*/*H* = 6 and *L*/*H* = 4. The amplification ratio is large in the high frequency range and the amplification ratio is larger in *L*/*H* = 6 than in *L*/*H* = 4. Consequently, the longer the dam crest length, the greater the acceleration generated at TB at the natural frequency in the high frequency range. It also confirms that the shorter the dam crest length, the amplification ratio of acceleration at TB becomes the smaller and the more influenced by the binding force of the abutment. And in *L*/*H* = 2, the natural frequency of the 1st mode has a frequency almost identical to the natural frequency of the 1st mode at TC. Therefore in *L*/*H* = 2, there is also vibration at TB during large vibration at TC and the same phenomenon occurs at TE. This result reveals that at the natural frequency of the 1st mode at TC in *L*/*H* = 2, the overall dam crest vibrates more than in the other models. The above results confirm that the effects of the binding force of the abutment have a strong effect on the frequency characteristics and that they appear abruptly between *L*/*H* = 4 and *L*/*H* = 2.

As shown in figure 11, in order to clarify these differences between the amplification ratios of acceleration in the longitudinal direction at the dam crest of the three models, the dimensionless quantities obtained by dividing the distances (ℓ) from the abutment of TC, TE, and TB by the half length of crest length (*L*/2) were adopted as the ratios of horizontal distance. The ratios of horizontal distance were 0 for the abutment, 0.33 for TB, 0.67 for TE, and 1 for TC. Figure 12 shows the relationships of the ratio of horizontal distance for each measurement point

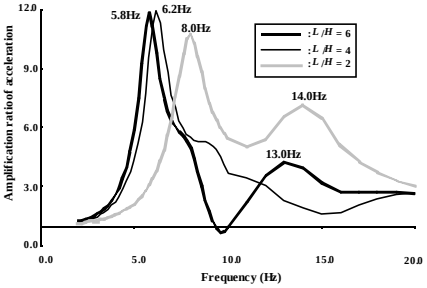

Figure 8: Resonance curves at TC

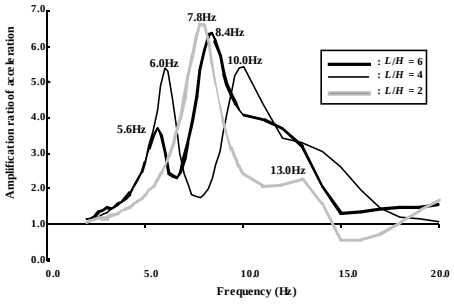

Figure 9: Resonance curves at TE

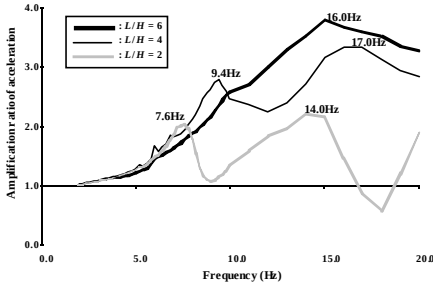

Figure 10: Resonance curves at TB

with the amplification ratio of acceleration at TC, TE and TB. The figure indicates that in L/H = 6, the acceleration amplified abruptly from TE to TC. In L/H = 2, the increment of amplification ratio was constant from TB to TC with no abrupt amplification observed. In addition, at TC, the amplification increased in the order L/H = 6, 4 and 2 but this sequence was reversed at TE and TB.

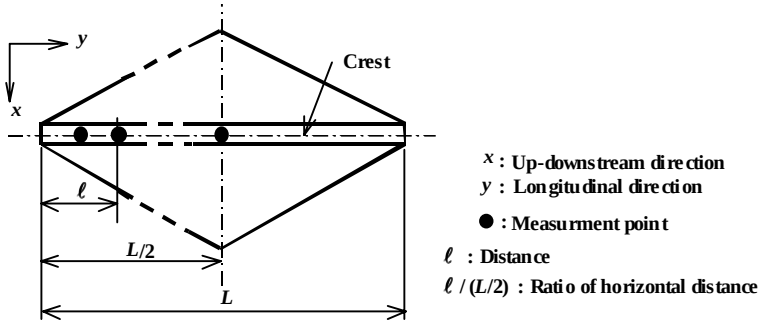

Figure 11: Definition of the ratio of horizontal distance

Photograph 2 shows the vibration modes in L/H = 2, L/H = 4, and L/H =6 respectively. Photograph 3 also shows magnified images of the vibration modes at the dam crest of each model. The dots on the dam crest are the measurement points of the displacement with the intervals of 10 cm. Figure 13 indicates changes in the maximum displacement in the longitudinal direction on the dam crest in the natural frequency of the 1st mode. The locations of the dots are defined as the ratios of horizontal distance as in fig. 11. This figure reveals tendencies almost identical to the change in the amplification ratio of acceleration at the dam crest shown in fig. 12. In L/H = 6, an abrupt increase in displacement occurs from TE to TC. In L/H = 4, the tendencies are similar to those of L/H = 6, but no abrupt increase in displacement is observed. In L/H = 2, displacement at TB is greater than in the other models, but no abrupt increase occurs. At TC, the displacement increases in the order L/H = 6, 4, and 2, but at TB the sequence is reversed so that the displacement increases in the order L/H = 2, 4, and 6.

Even the results of multi-strobe photography do not reveal a clear amplitude from the abutment to the TB in L/H = 4 and L/H = 6. In L/H =2, on the other hand, a clear amplitude is observed between the abutment and TB.

These results indicate that if L/H is small, deformation occurs throughout the dam crest but if L/H is large, deformation is large at the center on the dam crest.

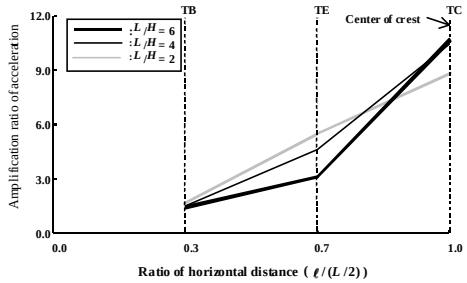

Figure 12: Amplification ratios of accelerations on dam crest

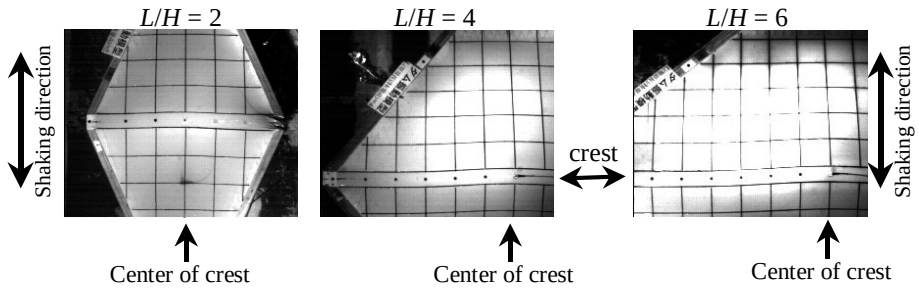

Photograph 2: Vibration modes of L/H = 2, 4 and 6

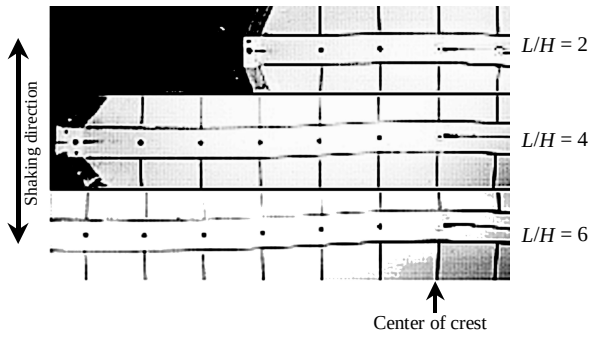

Photograph 3: Vibration modes on crest of *L*/*H* = 2, 4 and 6

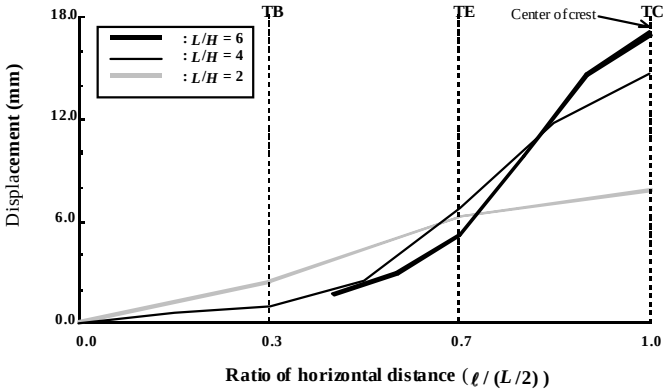

Figure 13: Maximum displacement on dam crest

Changes in the acceleration amplification and maximum displacement in the longitudinal direction on the dam crest reveal that when *L*/*H* is small, greater response acceleration and deformation are generated near the abutment than when *L*/*H* is large. From this fact, it can be assumed that greater discontinuous fluctuation of the response acceleration and the deformation occur near the connection between the abutment and dam body when *L*/*H* is small. It demonstrates that the ratio between *L*/*H* = 4 and *L*/*H* = 2 can be one standard determining whether large response acceleration and deformation are generated near the abutment.

NUMERICAL SIMULATION OF THE SHAKING TABLE TEST

As shown in figs 5, 6 and 7, it is clear that the dam models used for the tests are elastic bodies without dependency on the size of the input acceleration from 25 to 200 Gal. It is, therefore, possible to use a linear analysis method. Three-dimensional seismic response analysis based on a mode superposition method was employed to compare the vibration modes obtained from the high speed video photography of the models. This analysis uses an analysis code (code name = POETICS) developed by the authors [Yasunaka and Masukawa, 1992].

The material parameters for dynamic analysis were Young's modulus of 45.1 MN/m^2, Poisson's ratio of 0.499, and density of 1.036 g/cm^3. The Newark β method was used for the numerical integration that obtained the response for each mode. It did not account for damping because it was used to clarify differences between vibration modes that occur under the effects of the *L*/*H* ratio. The input waveform was a sine wave for the natural frequency of the 1st mode at each model and, it was input only in the upstream-downstream direction.

COMPARISON OF THE TEST RESULTS WITH THE ANALYSIS RESULTS

Figure 14 shows the vibration modes of the 1st order eigenfrequency based on their relationships with the ratios of horizontal distance defined by fig. 11. Eigen vector of the ordinate in Fig. 14 is converted to the dimensionless quantities. This figure reveals that the shape of the vibration mode in *L*/*H* = 2, unlike those in the other two models, is also deformed near the abutment and deformation occurs in the overall dam crest. This indicates that as *L*/*H* increases from 2 to 4 and then to 6, the deformation increases abruptly near the center on the dam crest.

Compared with Fig. 13, this result shows that three-dimensional response analysis based on the mode superposition method can be used to simulate the vibration properties of dam models.

In the results of the tests and the analysis, the vibration properties in L/H = 2 differ from those in L/H = 4 and L/H = 6. And in L/H =2, large response acceleration and deformation appear in the dam body near the abutment. This result suggests that in order to study the seismic behavior of a dam that is smaller ratio than L/H from L/H = 2 to L/H = 4, it is necessary to perform three-dimensional seismic response analysis.

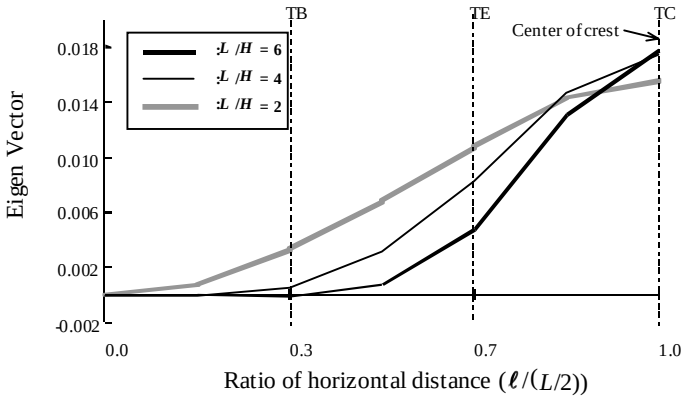

FIGURE 14: VIBRATION MODES ON CREST

Table 1 shows the eigenfrequencies obtained analytically. On the table, the directions of the obtained vibration modes are recorded under the eigenfrequencies. The lines under the vibration mode directions indicate the most dominant direction. This table indicates the eigenfrequencies in the high frequency range for L/H = 2. In L/H = 6, eigenfrequencies in the low frequency range are indicated. The same trends as in L/H = 6 are characteristic of L/H = 4.

From these results, it is deduced that the effects of the binding force of the abutment have a strong influence on both the shape of the vibration mode and the eigenfrequency.

Table 1: Eigenfrequencies up to the 6th order

The frequency of parenthesis: the natural frequency of dam model, underline: dominant mode

Order	L/H=2	L/H=4	L/H=6
1	7.97Hz (8.0Hz) Up-downstream	6.40Hz (6.2Hz) Up-downstream	5.95Hz (5.8Hz) Up-downstream
2	11.27Hz Up-downstream	8.20Hz Up-downstream	7.19Hz Up-downstream
3	13.27Hz (14.0Hz) Up-downstream + Vertical	9.56Hz (10.0Hz) Up-downstream	8.02Hz (8.4Hz) Up-downstream
4	13.54Hz Up-downstream + Vertical	9.85Hz Longitudinal + Vertical	8.31Hz Longitudinal + Vertical
5	14.59Hz Up-downstream + Longitudinal	10.63Hz Up-downstream	8.67Hz Up-downstream
6	14.85Hz Up-downstream + Longitudinal + Vertical	11.32Hz Up-downstream + Vertical	8.91Hz Up-downstream

CONCLUSION

Our tests and analyses revealed the following facts.

The resonance curves obtained from the shaking table tests indicate that at the natural frequency of the 1st mode, in L/H = 2, response acceleration amplifies at the entire dam crest, while in L/H = 4 and L/H = 6, it concentrically amplifies at the center on the dam crest. They also indicate that in L/H = 2, the shape of the 1st vibration mode differs from those of the other two models. This clearly shows that the effects of the binding force of the abutment are strongly expressed by the natural frequency and the shape of the vibration mode rather than by the amplification of the acceleration. It also indicates that the effects on the vibration properties of the binding force of the abutment appear abruptly between the L/H of 4 and 2.

The deformation patterns of the vibration modes obtained from the tests indicate tendencies almost identical to those of the acceleration amplification and that in L/H = 2, large displacement occurs near the abutment. They also indicate that in L/H = 6 and L/H = 4, displacement abruptly increases near the center on the dam crest. It is also clear that when L/H is small, the deformation of the vibration mode occurs throughout the dam crest and when L/H is large, the deformation of the vibration mode is large and dominant at the center on the dam crest.

The shape of the vibration mode of the analysis indicates that, as in the results based on the vibration testing, in L/H =2 deformation appears close to the abutment so deformation occurs throughout the dam crest unlike the other two models, and also shows that as L/H increases, deformation increases abruptly near the center on the dam crest. It also shows that the effects of the binding force of the abutment appear strongly in the shape of the vibration modes.

As explained above, changes in the amplification ratio of acceleration and the maximum displacement in the longitudinal direction on the dam crest indicate that when L/H is small, larger response acceleration and deformation occur near the abutment than when L/H is large. This result suggests the possibility that when L/H is small, greater discontinuous change of the response acceleration and deformation occurs near the connection of the abutment and the dam body. The results also suggest that it is necessary to perform three-dimensional seismic response analysis in order to study the seismic behavior of a dam whose L/H is smaller than L/H = 2 to 4.

REFERENCE

Masukawa, S., Yasunaka, M. and Tagashira, H. (1996), “Earthquake observation and three dimensional modal analysis of a rock fill dam”, *Proceedings 11WCEE*, No. 534.
Mejia, L. H. and Seed, H. B. (1982), “Comparison of 2-D and 3-D dynamic analyses of earth dams”, *Proceedings ASCE, Journal G. E.*, 109, 11, pp. 1383-1398.
Yasunaka, M. and Masukawa, S. (1992), “Seismic response analysis of a filldam with three-directional input of earthquake”, *Proceedings 10WCEE*, 8, pp. 4713-4718.